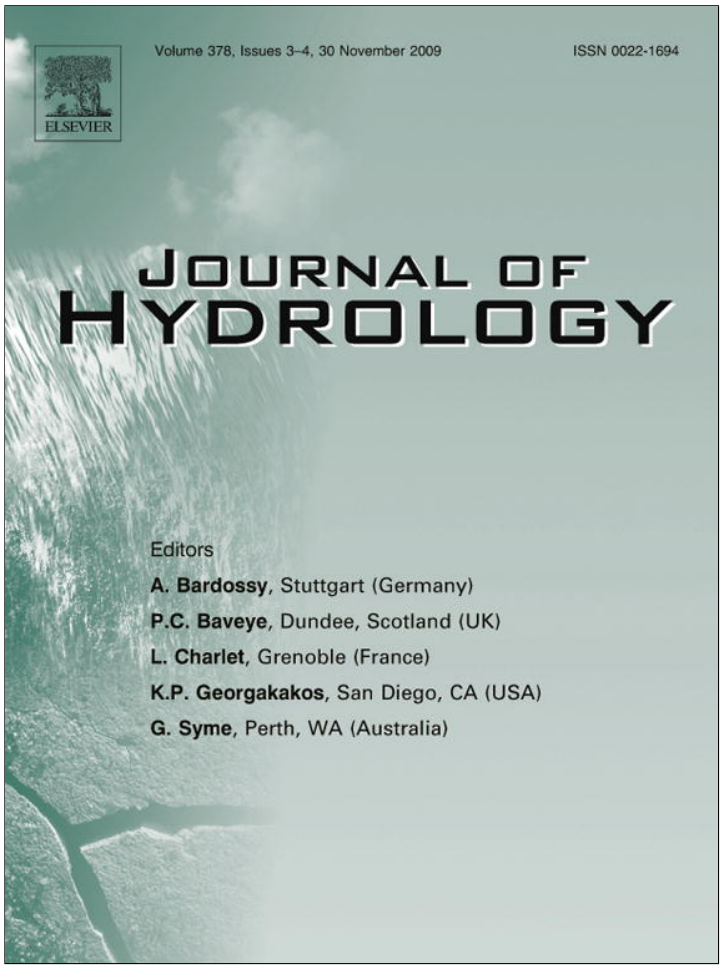

Journal of Hydrology 378 (2009) 343–354

Contents lists available at ScienceDirect

Journal of Hydrology

journal homepage: www.elsevier.com/locate/jhydrol

Simplified modeling of phosphorus removal by vegetative filter strips to control runoff pollution from phosphate mining areas

Y.-M. Kuo [a,b], R. Muñoz-Carpena [a,*]

[a] Agricultural and Biological Engineering Department, University of Florida, 101 Frazier Rogers Hall, PO Box 110570 Gainesville, FL 32611-0570, USA
[b] Department of Design for Sustainable Environment, MingDao University, 369 Wen-Hua Rd., Peetow, Chang-Hua 52345, Taiwan, ROC

ARTICLE INFO

Article history:
Received 10 November 2008
Received in revised form 8 September 2009
Accepted 24 September 2009

This manuscript was handled by L. Charlet, Editor-in-Chief, with the assistance of Ewen Silvester, Associate Editor

Keywords:
Sediment
Phosphorus
Mining sand tailings
Apatite
Vegetative filter strips
Uncertainty

SUMMARY

Runoff non-point source pollution from phosphate mining areas poses a potential risk to ecosystems in many parts of the world. Mining sand tailings in Central Florida, which still contain apatite (phosphate rock), have shaped the landscape in reclaimed lands at the upper Peace River basin. The objective of this study is to model the efficiency of vegetative filter strips for controlling surface runoff pollution from phosphate mining sand tailings. The numerical model VFSMOD-W is used to predict overland flow and sediment trapping within the filter and is linked to a simplified phosphorous (P) transport algorithm based on experimental data to predict total P (TP), particulate P (PP) and dissolved P (DP) fractions in the filter outflow. An advanced global inverse optimization technique is used for the model calibration process, and the uncertainty of the measured data is considered in goodness-of-fit indicators. The VFSMOD-W can predict hydrology and sediment transport well (Nash–Sutcliffe coefficient of efficiency >0.6) for calibration and validation events with peak outflow rate from VFS greater than 0.0004 m^3/s. The good prediction in runoff and sediment resulted also in good predictions of PP and TP transport since apatite is a main component of sediment. A good prediction of DP was found by considering the rainfall impact on DP dissolved from apatite in surface soil. The uncertainty of measured data included in the goodness-of-fit indicators is a more realistic method to evaluate model performance and data sets. VFSMOD-W combined with the simplified P modeling approach successfully predicted runoff, sediment, and P transport in phosphate mining sand tailings, which provides management agencies a design tool for controlling runoff and P transport using vegetative filter strips.

Introduction

Florida is rich in phosphate rock formed millions of years ago under ocean waters. Phosphate is a key ingredient in fertilizer and cannot be synthesized; so natural phosphate mining is the only supply and for the last 120 years has been one of the main economic activities in the Florida region. The extraction and beneficiation of phosphate rock to produce fertilizer has the potential to adversely impact the environment. Mining impacts the landscape and can lead to water contamination, excessive water consumption, and air pollution (UNEP, 2001). The continued mining activities in Central Florida have degraded water quality in the upper Peace River basin and have left behind large refuse sand tailings that now shape the landscape surrounding the river. The mound material is essentially homogenous clean sand (>94% of soil weight) with a high concentration of apatite, the phosphorus (P) mineral ore, and is mixed with small pockets of clay in some areas. The average dissolved P (DP) concentration of runoff water measured in the Peace River at the Bartow sub-basin ranged from 0.4 to 3.0 g/m^3 in 2006 (Kuo, 2007). These values are higher than the maximum allowable total P (TP) concentration of 0.1 g/m^3 discharging into a river established by the US Environmental Protection Agency (USEPA, 2000; Mueller et al., 1995). Thus, reclamation activities must be conducted to avoid continued environmental impacts in this and other phosphate mining areas around the world.

The reclamation activities in mining areas generally involve landscaping, planting vegetation, and maintenance of disturbed areas (UNEP, 2001). Planting vegetation can be an economical and less laborious method. Vegetation can increase surface roughness and infiltration, and decrease runoff volume that can reduce particles and sediment bound pollutant transport. Vegetative filter strips (VFS) are defined as areas of vegetation designed to reduce transport of sediment and pollutants from surface runoff by deposition, infiltration, adsorption, and absorption (Dillaha et al., 1989). VFS has been recommended as a best management practice (BMP) in controlling non-point source pollution from disturbed lands (USDA-NRCS, 1976; Barfield et al., 1979).

* Corresponding author. Tel.: +1 352 3921864x287; fax: +1 352 3924092.
E-mail addresses: airkuo@ntu.edu.tw (Y.-M. Kuo), carpena@ufl.edu (R. Muñoz-Carpena).

0022-1694/$ - see front matter © 2009 Elsevier B.V. All rights reserved.
doi:10.1016/j.jhydrol.2009.09.039

In a previous study, field experiments of surface runoff P transport from vegetative filter strips (VFS) and disturbed areas were conducted in sand tailings (Kuo et al., 2005). For this purpose, fully instrumented runoff plots were constructed at different locations in the Peace River basin representing the range of conditions found in the region (landscape slope and lengths, soil variability, locally recommended grasses, climate characteristics, etc.). Their results observed from forty rainfall–runoff events at two sites showed that VFS effectively reduce surface pollution transport in this phosphate mining area. Compared to the amounts measured from the bare sand tailings, reduction in runoff volume (Q), sediment load, TP, and DP at the VFS outflow was at least 62%, 97%, 96%, and 66%, respectively, for all the events studied (Kuo, 2007).

Mathematical models for simulating water and/or sediment transport in VFS can be good tools for assessing the impacts of human activities and natural processes on water resources and for designing optimal BMPs to reduce these impacts. One such model is VFSMOD-W, developed by Muñoz-Carpena et al. (1999), which simulates water and sediment transport in vegetated filter strips based on an advanced finite elements solution of the kinematic wave overland flow equation (Muñoz-Carpena et al., 1993a), Einstein bed load sediment transport equation (Barfield et al., 1978), suspended sediment transport (Tollner et al., 1976), and infiltration into the soil matrix (Muñoz-Carpena et al., 1993b).

VFSMOD-W infiltration, outflow and sediment trapping efficiency components have been successfully tested with field data from the North Carolina's Coastal Plain (Muñoz-Carpena et al., 1993a,b) and Piedmont (Muñoz-Carpena et al., 1999), Midwest (Fox et al., 2005; Sabbagh et al., 2009; Poletika et al., 2009), Canada (Abu-Zreig et al., 2001; Gharabaghi et al., 2000), and Germany (Sabbagh et al., 2009). The model has been used to estimate successfully other pollutant reduction processes like pesticide reduction (Sabbagh et al., 2009; Poletika et al., 2009), P-yield reduction (Rudra et al., 2002), and total suspended sediment removal from an experimental VFS treating highway runoff (Han et al., 2005). VFSMOD-W has also been applied to simulate fecal pathogen filtering from runoff (Zhang et al., 2001), to construct field VFS design aids (Dosskey et al., 2008); and conjugated with other spatially distributed tools like AnnAGNPS (Yang and Weersink, 2004), SWAT (White and Arnold, 2009) and others (Kizil and Disrud, 2002; Dosskey et al., 2005, 2006; Tomer et al., 2009). The US-EPA (Kalin and Hantush, 2003; USEPA, 2005) listed VFSMOD-W as one of the models to evaluate the efficiency of the BMP in VFS for protecting watershed environments. VFSMOD-W has also been identified as a potential BMP design tool for reducing surface P runoff from the reclaimed phosphate mines in Florida (specifically in Polk County) and other similar areas elsewhere.

The success in modeling hydrological and water quality processes heavily depends on the quality of the model parameters, i.e. to ensure that they are representative of the hydrologic properties (climate, soil and vegetation) for a specific application. Thus, the first step of applying VFSMOD-W in predicting VFS treatment of runoff from mining tailings is to identify optimal model parameters. A popular method for parameter estimation is manual calibration by a "trial and error" procedure comparing simulated values with measured values. However, this method is time consuming, quite subjective, and cannot ensure that the best parameter set is found. A more elaborate, complex and increasingly attractive form of parameter estimation is inverse optimization. This procedure can provide effective parameters in the range of the envisaged model application, and overcomes the drawbacks of manual calibration (Ritter et al., 2003).

In addition, in order to model hydrological processes successfully, uncertainty in the model predictions should be taken into account (Beven, 2006). One source of model uncertainty is associated with the uncertainty of measured data, which can result from field measurements, water sample collection and storage, and water quality chemical analysis (Harmel et al., 2006). Thus, a more realistic evaluation of model performance is achieved by including the uncertainty of measured data in model goodness-of-fit indicators used during the model testing process.

In this study the efficiency of VFSs to control surface runoff pollution from phosphate mining sand tailings was simulated using the numerical model VFSMOD-W. Overland flow and sediment trapping predictions within the filter were linked with a simplified P transport algorithm based on experimental data to predict total, particulate and dissolved P fractions at the filter outflow. The inverse optimization technique was used for the model calibration process, and the uncertainty of the measured data was considered in the goodness-of-fit evaluation of different model output quantities.

Materials and methods

Field experiments

The experimental site is located on a former phosphate mining area, on the property of the Bureau of Mine Reclamation, Florida Department of Environmental Protection (FDEP), Bartow, in Central Florida. Two experimental sites (site A and site B) 3 km apart were chosen to represent the bare disturbed sand tailings often found in the upper Peace River watershed. A sketch of the experimental setup at both plots is shown in Fig. 1. At each site, four VFSs were established and their corresponding source areas were delimited with a border made of aluminum siding plates of 40 cm width inserted vertically in the ground 20 cm below the surface. This allowed for testing different source-to-VFS area ratios. Average slopes at site A and site B were 2.0%, and 4.3%, respectively, while the lengths of the source areas at both sites were 14.4 m and 40.0 m, respectively. Two different VFS lengths were used at each site: 4.1 m and 5.8 m at site A and 6.8 m and 13.4 m at site B, respectively. All source areas and VFSs presented a width of 3.3 m. Thus, the source-to-VFS area ratio for the two filters at site A were 2.5 and 3.5, while at site B, these were 3.0 and 6.0. The main vegetation in the filter areas is Bahia grass, which accounts for about 90%, and the remaining vegetation is composed of Hairy Indigo, Cogon grass, and Smutgrass. Kuo (2007) determined the grass spacing by counting the amount of grass stems within a 0.5 m by 0.5 m frame thrown randomly on the grass surface. Each VFS and source area were fully instrumented to monitor rainfall, soil moisture, runoff and sediment load at the filter inflow and outflow (Fig. 1). Runoff was collected with a rain gutter buried at the outlet of each source area from where it flowed into a flume and sampling trough. Then, runoff was redistributed through a perforated PVC spreader installed at the entry of the corresponding VFS. A cover was installed to prevent direct rain from falling into the runoff gutter. During each rainfall event, flow rate was measured with 6 in. (15.24 cm) HS flumes provided with a capacitance probe (ECH_2O, model EC-20, Decagon Devices, WA) inserted vertically in the throat of each flume to obtain the stage. Using the appropriate calibration equation, a field datalogger (CR-10X, Campbell Scientific, UT) was programmed to record flow rate from the capacitance probe in each flume every minute. Additionally, runoff water samples were collected at each trough positioned below the flume outlet by an automatic water sampler containing 24 plastic sampling bottles (ISCO 6712, ISCO, Inc.). The datalogger was configured in order to send pulses to the ISCO 6712 automatic water sampler based on changes in accumulated runoff volume recorded at each flume such that the 24 samples were distributed throughout the runoff event. After activation, the sampler purged the suction hose and then collected runoff water samples from the sampling trough into the 500 mL bottles. Runoff samples were brought to laboratory and

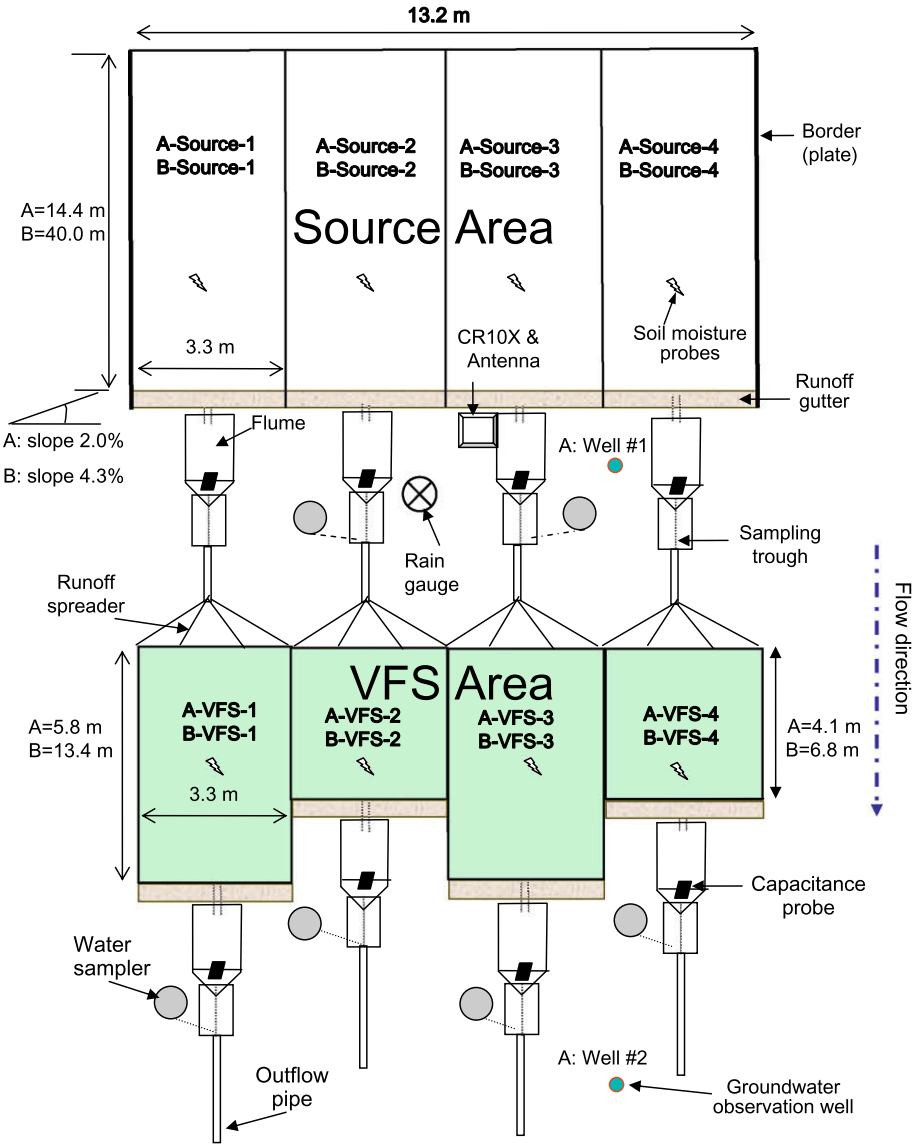

Fig. 1. Schematic diagram of the experimental sites (sites A and B) in Bartow, FL. A: site A; B: site B.

analyzed for concentrations of sediment, TP, and DP. Loads and flow-weighted mean concentration were computed for each collected event.

Field data at site A were collected during the entire 2006, while at site B data were collected during the rainy season, from June to December. A total of twenty four events with over 300 runoff water samples were collected from these two sites to test VFSMOD-W performance. Hyetograph, and inflow and outflow hydrographs and pollutographs (sediment, TP, and DP) were recorded for each event.

Simplified phosphorus modeling

P transport in the VFS was modeled by separately computing the concentration of dissolved P (DP) and particulate P (PP). According to Kuo (2007), the latter can be calculated from the outflow sediment concentration, such that:

$$[PP] = 0.02606 \cdot [Sed] \quad \text{with } R^2 = 0.988, \tag{1}$$

where square brackets indicate concentration, i.e. [*PP*] and [*Sed*] are the concentration (kg/m^3) of particulate P and sediment, respectively. This experimental equation (slope = 0.02606) is in agreement with the TP content found in the soil samples (2.3% of soil weight). Table 1 shows that the finer particle classes contain higher P concentration. Trapping of coarse fractions within the filter results in a relative enrichment in fine particles in the sediment outflow from the VFS; thus, the ratio in Eq. (1) is higher than the TP fraction in the soil surface. Eq. (1) is deemed valid not only because it provided a high goodness-of-fit coefficient (R^2 = 0.988), but also because the data used for its development embodies a wide range of experimental conditions (different locations with soil types, slopes, field and buffer lengths, and precipitation and runoff intensities) representative of the *P* mining tailings found in the area.

Two alternative approaches were tested to simulate DP transport in the VFS. The first approach proposes that dissolution of P from apatite in soil and sediment is an important component controlling DP concentration in the filter runoff. Kuo (2007) and Kuo et al. (2009) found that a high equilibrium P concentration at zero net P sorption for soils from both sites (approximately 11–15 mg L^{-1}) is much higher than all runoff DP concentrations (0.4–3.0 mg L^{-1}) analyzed from at least 300 runoff water samples collected at the sites. This indicates that runoff samples were

Table 1
P concentrations in different particle size classes. Data are average ± standard deviation values of four samples within each plot.

Site	Plot	P concentrations (mg/kg) in each particle size class (μm)				
		0.45–2	2–37	37–100	100–250	250–2000
A	Source	29,560 ± 2030	28,973 ± 2230	20,295 ± 2670	17,618 ± 1660	15,634 ± 1890
	VFS	32,051 ± 2080	30,749 ± 1430	21,780 ± 860	19,594 ± 1610	17,020 ± 1240
B	Source	30,813 ± 1800	29,660 ± 2270	23,294 ± 1920	19,937 ± 1350	16,503 ± 1170
	VFS	32,318 ± 2200	31,158 ± 1580	24,669 ± 1770	19,766 ± 2020	16,762 ± 1450

undersaturated with respect to apatite. In addition, a strong relationship was found between calculated apatite specific surface area and measured DP concentration in water extracts. These findings support that apatite dissolution is a major factor controlling P release from these soils, and that the soil and sediment act as a long-term source of P in runoff, rather than a sink (through P sorption). Since the runoff solution is undersaturated in DP, we can assume that measured inflow and outflow DP concentrations in the VFS are similar, $[DP]_{in} \approx [DP]_{out}$. Thereby, the outflow DP mass (DP_{out}, kg) can be computed as:

$$DP_{out} = \sum_{l=1}^{n} V^l_{out}[DP]^l_{in} \tag{2}$$

where $[DP]^l_{in}$ is the DP inflow concentration (kg/m^3); and V^l_{out} the runoff outflow volume (m^3), both at time step l. Furthermore, assuming a dynamic equilibrium of DP mass within the VFS, the mass balance at the end of each rainfall–runoff event can be established, such that the DP outflow mass (kg) may result from the inflow mass plus the P contribution by rainfall plus the P release from apatite minus the amount of P lost by infiltration as shown in the following equation:

$$DP_{out} = DP_{in} + DP_D + DP_{rain} - DP_F \tag{3}$$

The subscripts "*out*" and "*in*" indicate the outflow and inflow masses, respectively; "*D*" represents the mass released from apatite; and "*rain*" and "*F*" indicate the mass contained in the rainfall and that infiltrated into soil, respectively. Assuming that $DP_{rain} = 0$ and $[DP]_{in} \approx [DP]_{out}$, Eq. (3) can be expressed as:

$$DP_{out} = \sum_{l=1}^{n} V^l_{out}[DP]^l_{in} = \sum_{l=1}^{n} \left(V^l_{in}[DP]^l_{in} + V^l_{out}[DP]^l_D - V^l_F[DP]^l_{in} \right) \tag{4}$$

where $[DP]^l$ and V^l indicate DP concentration (kg/m^3) and runoff volume (m^3) at time step l, respectively. By considering the water balance $V^l_{out} = V^l_{in} + V^l_{rain} - V^l_F$ and substituting into Eq. (4) it follows that

$$[DP]^l_D = V^l_{rain}[DP]^l_{in}/V^l_{out} \tag{5}$$

Eq. (5) suggests that the DP concentration as a result of apatite dissolution is related to rainfall, inflow DP concentration, and outflow rate. Thus, DP released from apatite may result from the impact of rainfall intensity as proposed by Gao et al. (2004).

The second approach does not take into account the dissolution of apatite, and the mass contribution by rainfall is neglected ($DP_D = 0$ and $DP_{rain} = 0$ in Eq. (3)). Under the assumption that the inflow DP concentration is diluted due to rainfall, and then the diluted DP concentration infiltrates into soil, the outflow DP mass can be computed as:

$$DP_{out} = \sum_{l=1}^{n} (V^l_{in}[DP]^l_{in} - (V^l_{in}/(V^l_{in} + V^l_{rain}))V^l_F[DP]^l_{in}) \tag{6}$$

By considering the water volume balance ($V^l_F = V^l_{in} + V^l_{rain} - V^l_{out}$), Eq. (6) is reduced to:

$$\begin{aligned} DP_{out} &= \sum_{l=1}^{n} ((V^l_{in}V^l_{in} + V^l_{in}V^l_{rain} - V^l_{in}(V^l_{in} + V^l_{rain} - V^l_{out})) \\ &\quad /(V^l_{in} + V^l_{rain}))[DP]^l_{in}DP_{out} \\ &= \sum_{l=1}^{n} (V^l_{in} \cdot V^l_{out}/(V^l_{in} + V^l_{rain}))[DP]^l_{in} \end{aligned} \tag{7}$$

Thereby, the importance of DP dissolution from apatite due to rainfall impact may be established by comparing DP_{out} computed with both Eq. (2) and Eq. (7).

Inverse calibration methodology and model validation

To test VFSMOD-W performance, rainfall–runoff experimental events were divided into calibration and validation events. The calibration of the hydrology component was done first as the sediment component builds on these results.

Calibration procedure

The flow or sediment parameters were estimated using inverse modeling by minimizing the following objective function:

$$OF(\vec{b}) = \sum_{i=1}^{N} w_i[O(t_i) - P(t_i, \vec{b})]^2 \tag{8}$$

where $OF(\vec{b})$ is the objective function of parameter vector $\vec{b}$ that represents the error between measured and simulated values; $O(t_i)$ and $P(t_i)$ are observed and predicted values (hydrographs or sedimentographs) using parameter vector $\vec{b}$, respectively; t is the time; N is the number of measurements available; and w_i is the weight of a particular measurement (Lambot et al., 2002). VFSMOD-W was coupled with the Global Multilevel Coordinate Search (GMCS) algorithm (Huyer and Neumaier, 1999) combined sequentially with the classical Nelder–Mead Simplex (NMS) algorithm (Nelder and Mead, 1965) (GMCS-NMS) to perform the inverse calibration of parameter vector $\vec{b}$ (Ritter et al., 2007). The GMCS can deal with objective functions with complex topography and has the advantage that initial values of the parameters to be optimized are not needed. The NMS method (also known as downhill simplex method) refines the locally optimal solution to a nonlinear problem with several variables when the objective function varies smoothly. From Kuo (2007) it follows that the inverse modeling algorithm integrated in the VFSMOD-W is robust since it successfully calibrated the parameters even in the presence of random noise associated with the measured data.

Selected calibrated parameters

The main parameters of hydrology and sediment transport that can be used in model calibration are listed in Table 2. The sensitive parameters were chosen based on an initial sensitivity analysis (Muñoz-Carpena et al., 2007). These authors performed a global sensitivity analysis to gain insight in the dependence of the VFSMOD-W outputs on certain model input factors, i.e. the most important

Table 2
Simulation parameters for the VFSMOD-W.

No	Parameter	Description	Value	Units
Hydrology component				
1	FWIDTH	Effective flow width of the strip	3.3	m
2	VL	Length of the filter (flow direction)	4.1–13.4	m
3	RNA	Filter Manning's roughness coefficient	0.1–0.45	$s/m^{1/3}$
4	SOA	Filter slope	0.02–0.05	m/m
5	VKS	Saturated hydraulic conductivity in the VFS	1.0×10^{-6}–1.1×10^{-4}	m/s
6	SAV	Green–Ampt's average suction at wetting front	0.22–0.43	m
7	OS	Saturated soil water content	0.37–0.49	m^3/m^3
8	OI	Initial soil water content	0.05–0.25	m^3/m^3
9	SM	Maximum surface storage	0	m
10	SCHK	Relative distance from the upper filter edge where check for ponding conditions is made (i.e. 1 = end, 0.5 = mid point, 0 = beginning)	0	–
Sediment component				
11	SS	Average spacing of grass stems	3.7–4.2	cm
12	VN	Filter media (grass) modified Manning's coefficient (0.012 for cylindrical media)	0.01–0.076	$s/cm^{1/3}$
13	H	Filter grass height	16.5–18.0	cm
14	VN2	Bare surface Manning's coefficient for sediment inundated area in grass filter	0.04	$s/m^{1/3}$
15	d_p	Sediment particle size diameter (d_{50})	0.011–0.041	cm
16	COARSE	Fraction of incoming sediment with particle diameter > 0.0037 cm (coarse fraction routed through wedge as bed load) [unit fraction, i.e. 100% = 1.0]	0.58–0.85	–
17	CI	Incoming flow sediment concentration	0.004–0.035	g/cm^3
18	POR	Porosity of deposited sediment	0.434	m^3/m^3
19	SG	Sediment particle density	2.65	g/cm^3

model parameters, and reported that for the same conditions as those of our experimental area, the saturated hydraulic conductivity (VKS) is a main factor in dominating the overland flow through the filter. Variations in the Manning's roughness coefficient (RNA) mainly controlled the time to peak of the outgoing hydrograph and had little effect on sediment output (Muñoz-Carpena et al., 1999). The porosity may change during the vegetation growing season, since plant roots may compact soil or break up soil matrix which will affect saturated water content (OS) and VKS. Therefore, calibration of the hydrology component was performed by optimizing VKS, OS, and RNA to match the observed outflow hydrograph.

The order of important parameters with respect to sediment transport was median of sediment particle size (dp), effective filter strip flow width (FWIDTH), VKS, and grass modified Manning's coefficient (VN). FWIDTH was fixed according to field measurement. Only dp and VN were chosen to calibrate the sediment component and then to validate events from the second filter length for the same experimental site. Once the parameters of the hydrology component were optimized, the sediment component was calibrated following the same approach by optimizing VN and dp to match the predicted and observed sediment outflow graph. No hydrology inputs were modified during this process.

Measurements of selected parameters

In order to obtain initial information of the parameters selected for optimization, VKS, Green–Ampt's average suction at wetting front (SAV), OS, and d_p were measured. Core cylinders made of brass with 5.4 cm diameter and 6.0 cm height (Soil moisture Equipment Corp, CA) were used to collect undisturbed soil samples. The soil cores were then saturated with 0.005 M $CaSO_4$-thymol solution and the saturated hydraulic conductivity (VKS) was measured based on the application of Darcy's Law with a constant head permeameter (section 3.4.2.2 in Dane and Topp, 2002). Saturated and final weights of the soil were measured and used to calculate bulk density and soil porosity (OS). The average suction at the wetting front (SAV) was also estimated as the area under the unsaturated hydraulic conductivity curve from the Millington and Quirk (1960) procedure by applying the *SoilPrep* model (Workman and Skaggs, 1990). Initial water content (OI) was measured using a capacitance probe (ECH_2O, model EC-20, Decagon Devices, WA) for each event. Equipment employing the "Polarization Intensity Differential Scattering" technique (Beckman-Coulter, Inc.) was used to analyze particle size distribution of soil and sediment samples (d_p). In addition, VN and RNA values were estimated from Haan et al. (1994) and Foster et al. (1980), respectively. Mean value and measured range of each parameter selected for calibration are given in Table 3. Since a limited number of measured values for each parameter is often insufficient to represent the field variability, the calibration range for each parameter was set to wider or equal the measured range. Table 4 defines the model output quantities (QPF, TRF, MSF, RDR, SDR, PPF, DPF, and TPF) used to evaluate the model's performance based on predicted and measured results.

Table 3
Parameter measured values and ranges used in the VFSMOD-W model calibration.

Component	Parameter[a]	Site A			Calibrated Range	Site B			Calibrated Range
		Measured				Measured			
		n	Mean	Range		*n*	Mean	Range	
Hydrology	VKS	8	5.6×10^{-5}	1.0×10^{-6}–1.1×10^{-4}	1.0×10^{-6}–1.1×10^{-4}	8	1.8×10^{-05}	1.0×10^{-6}–1.1×10^{-4}	1×10^{-6}–1.1×10^{-4}
	OS	8	0.41	0.37–0.46	0.32–0.54	8	0.46	0.40–0.49	0.32–0.57
	RNA[b]	–[d]	–	0.10–0.45	0.05–0.50	–	–	0.10–0.45	0.05–0.50
Sediment	VN[c]	–	–	0.010–0.074	0.010–0.074	–	–	0.010–0.074	0.010–0.074
	d_p	10	0.0207	0.0094–0.0286	0.0038–0.030	20	0.0210	0.0150–0.030	0.0038–0.030

[a] Units of parameters are shown in Table 2.
[b] Foster et al. (1980).
[c] Haan et al. (1994).
[d] No value provided.

Table 4
Selected output quantities of hydrology, sediment, and phosphorus transport.

Quantity	Units	Description
Hydrology		
TRF	m^3	Total runoff output from filter
QPF	m^3	Peak flow in outflow from filter
RDR	–	Runoff delivery ratio
Sediment		
MSF	kg	Mass of sediment output from filter
SDR	–	Sediment delivery ratio
Phosphorus		
DPF	g	DP mass output from filter
PPF	g	PP mass output from filter
TPF	g	TP mass output from filter

Validation procedure

Validation was carried out for the selected validation events by running the model for the second filter length in each site with the parameters obtained from the calibration run (modifying only the measured length and slope on the filter, incoming hydrograph, and initial soil moisture for hydrology and only CI for sediment) and comparing the results with the observed data for that filter.

Goodness-of-fit indicators

The goodness-of-fit indicators were used to evaluate the performance of the model simulation during the calibration and testing processes. The Nash–Sutcliffe coefficient of efficiency (C_{eff}, Nash

Table 5
Measured data uncertainty of DP, TP, sediment, and flow for each category.

Measured item	E_1 = Flow[a]		E_2 = Sampling[b]		E_3 = Storage[c]		E_4 = Analysis[d,e]		PER (%)
	Range (%) (central value)	Used (%)	Range (%) (central value)	Used (%)	Range (%) (central value)	Used (%)	Range (%) (central value)	Used (%)	
DP	−5 to 10 (–)[h]	20	0 to 0 (0)	0	−39 to 20 (−17)	45[f]	−14 to 22 (8)	8	50
TP	−5 to 10 (–)	20	0 to 17 (0)	20[g]	−64 to 9 (−11)	11	−24 to 22 (2)	2	30
Sediment	−5 to 10 (–)	20	14 to 33 (20)	20	0 to 0 (0)	0	−4.9 to −2.5 (–)	5	29
Flow	−5 to 10 (–)	20	0 to 0 (0)	0	0 to 0 (0)	0	0 to 0 (0)	0	20

[a] Sauer and Meyer (1992).
[b] Martin et al. (1992).
[c] Kotlash and Chessman (1998).
[d] Gordon et al. (2000).
[e] Mercurio et al. (2002).
[f] Sampling error taken as that of sediment since most P in TP comes from mineral apatite in sediment.
[g] Storage taken as maximum value (39%) but increased up to 45% to account for potential dissolution of apatite.
[h] No value provided.

Table 6
Calibrated parameters for hydrology and sediment model components, and measured and predicted output quantities.

Event ID	Hydrology			Sediment		Measured quantities								Predicted quantities						
	VKS (m/s)	OS (m)	RNA (s/$m^{1/3}$)	d_p (mm)	VN (s/$m^{1/3}$)	CI (g/cm^3)	QPF (m^3/s)	TRF (m^3)	MSF (kg)	DPF (g)	TPF (g)	RDR (%)	SDR (%)	QPF (m^3/s)	TRF (m^3)	MSF (kg)	DPF (g)	TPF (g)	RDR (%)	SDR (%)
Calibration																				
B061306V2[a]	0.000021	0.39	0.407	0.0053	0.024	0.0221	6.7×10^{-5}	0.020	0.001	0.035	0.064	3.86	0.02	1.0×10^{-4}	0.008	0.001	0.014	0.028	1.54	0.00
B071406V3	0.000010	0.54	0.082	0.0042	0.051	0.0340	7.6×10^{-4}	0.428	0.058	0.751	2.214	41.4	0.14	8.8×10^{-4}	0.259	0.018	0.586	1.055	25.0	0.03
B072006V3	0.000007	0.41	0.203	0.0054	0.042	0.0350	1.1×10^{-3}	0.887	0.149	1.511	6.390	73.4	0.35	2.0×10^{-3}	0.721	0.091	1.146	3.517	59.7	0.22
B072806V3	0.000012	0.54	0.128	0.0045	0.011	0.0220	3.9×10^{-4}	0.233	0.030	0.370	1.171	28.4	0.19	7.2×10^{-4}	0.073	0.002	0.094	0.146	8.89	0.01
B090606V2	0.000018	0.52	0.315	0.0061	0.044	0.0341	1.3×10^{-3}	0.287	0.049	0.520	1.812	43.8	0.22	1.3×10^{-3}	0.240	0.035	0.373	1.285	36.6	0.16
B090906V2	0.000011	0.56	0.267	0.0048	0.012	0.0120	2.4×10^{-3}	3.494	0.622	5.874	21.220	82.0	1.82	2.6×10^{-3}	3.324	0.552	5.366	19.75	78.0	1.08
B091006V3	0.000008	0.55	0.260	0.0050	0.030	0.0310	1.1×10^{-3}	0.940	0.119	1.233	3.758	55.7	0.23	1.4×10^{-3}	0.836	0.104	1.311	4.021	49.5	0.20
B101206V3	0.000019	0.47	0.173	0.0054	0.049	0.0324	9.7×10^{-4}	0.254	0.027	0.376	1.111	34.2	0.11	1.4×10^{-3}	0.189	0.011	0.277	0.563	25.4	0.05
A020306V3	0.000038	0.53	0.195	0.0070	0.053	0.0040	2.4×10^{-5}	0.020	0.000	0.005	0.010	1.86	0.00	2.7×10^{-5}	0.004	0.000	0.002	0.006	0.37	0.00
A070706V3	0.000019	0.36	0.137	0.0041	0.024	0.0180	8.9×10^{-4}	0.062	0.002	0.030	0.081	31.5	0.19	1.7×10^{-4}	0.040	0.000	0.017	0.029	20.3	0.01
A072806V3	0.000020	0.49	0.327	0.0061	0.075	0.0300	4.0×10^{-4}	0.143	0.009	0.059	0.380	45.1	0.47	8.8×10^{-4}	0.116	0.002	0.051	0.096	36.6	0.02
A091006V3	0.000028	0.43	0.425	0.0052	0.060	0.0125	6.3×10^{-5}	0.055	0.002	0.015	0.056	31.1	0.13	1.8×10^{-4}	0.023	0.000	0.011	0.023	13.0	0.02
Validation																				
B061306V3	0.000021	0.39	0.407	0.0053	0.024	0.0130	9.0×10^{-6}	0.006	0.000	0.007	0.011	3.17	0.02	$0.0 \times 10^{+0}$	0.000	0.000	0.000	0.000	0.00	0.00
B071406V2	0.000010	0.54	0.082	0.0042	0.051	0.0250	5.9×10^{-4}	0.323	0.059	0.958	2.220	25.0	0.16	1.1×10^{-3}	0.600	0.087	1.046	3.313	46.5	0.27
B072006V2	0.000007	0.41	0.203	0.0054	0.042	0.0300	1.6×10^{-3}	0.653	0.202	1.206	6.858	55.3	0.57	2.2×10^{-3}	0.842	0.213	1.019	6.569	71.3	0.60
B072806V2	0.000012	0.54	0.128	0.0045	0.011	0.0150	3.4×10^{-4}	0.154	0.010	0.234	0.460	26.0	0.14	1.0×10^{-3}	0.129	0.009	0.156	0.390	21.8	0.10
B090606V3	0.000018	0.52	0.315	0.0061	0.044	0.0300	2.2×10^{-5}	0.014	0.001	0.021	0.043	2.80	0.01	$0.0 \times 10^{+0}$	0.000	0.000	0.000	0.000	0.00	0.00
B090906V3	0.000011	0.56	0.267	0.0048	0.012	0.0175	2.1×10^{-3}	2.681	0.330	4.332	13.340	68.8	0.58	2.3×10^{-3}	2.614	0.268	4.123	11.11	67.1	0.39
B091006V2	0.000008	0.55	0.260	0.0050	0.030	0.0220	1.4×10^{-3}	1.028	0.127	1.942	5.019	55.2	0.31	1.6×10^{-3}	1.281	0.203	2.015	7.305	68.8	0.50
B101206V2	0.000019	0.47	0.173	0.0054	0.049	0.0340	1.9×10^{-3}	0.440	0.068	0.686	2.692	65.1	0.13	2.1×10^{-3}	0.386	0.094	0.503	2.953	57.1	0.41
A020306V2	0.000038	0.53	0.195	0.0070	0.053	0.0090	9.0×10^{-5}	0.050	0.002	0.014	0.075	5.20	0.06	1.5×10^{-4}	0.019	0.000	0.010	0.022	1.98	0.01
A070706V2	0.000019	0.36	0.137	0.0041	0.024	0.0250	1.1×10^{-4}	0.044	0.002	0.018	0.066	34.4	0.23	2.3×10^{-4}	0.055	0.002	0.014	0.054	43.0	0.05
A072806V2	0.000020	0.49	0.327	0.0061	0.075	0.0230	7.7×10^{-5}	0.027	0.000	0.007	0.018	9.34	0.02	5.8×10^{-4}	0.075	0.001	0.034	0.065	26.0	0.02
A091006V2	0.000028	0.43	0.425	0.0052	0.060	0.0120	5.1×10^{-5}	0.036	0.000	0.011	0.020	25.9	0.02	2.6×10^{-4}	0.033	0.000	0.017	0.018	23.7	0.00

[a] In Event ID, A = site A; B = site B; six numbers succession = Gregorian date; V2 = plot number 2 in VFS area. The lengths of V2 and V3 at site A are 4.1 m and 5.8 m, respectively, and at site B are 6.8 m and 13.4 m, respectively.

and Sutcliffe, 1970) and root mean square error (*RMSE*) are commonly used goodness-of-fit indicators to evaluate model performance (Legates and McCabe, 1999). However, the C_{eff} is not very sensitive to systematic model over- or under-prediction especially during low flow periods (Krause et al., 2005). To reduce the oversensitivity to extreme values in the C_{eff}, a modified form of C_{eff} (Krause et al., 2005), C_{eff_m}, was applied to evaluate potential systematic (e.g. over- or under-prediction) and dynamic (e.g. timing, and falling or rising lamb) model simulation errors. The detailed description of goodness-of-fit indicators is presented in the Appendix section. Using a combination of these indicators (C_{eff}, C_{eff_m}, and *RMSE*), an appropriate model performance evaluation can be conducted.

Consideration of measured data uncertainty in the model evaluation

Common sources of measured errors of hydrologic and water quality data are related to flow measurement, sample collection, sample storage, and laboratory analysis (Harmel et al., 2006). The deviation term ($e_i = O_i - P_i$) in goodness-of-fit indicators is normally determined as the difference between observed and predicted data. This deviation term does not account for uncertainty of measured data in indicators. Therefore, Harmel and Smith (2007) modified the deviation term in goodness-of-fit indicators based on the cumulative probable error to appropriately compare model predictions and observations.

The probable error range (PER) resulting from the various hydrologic/water quality data collection procedures can be estimated by the propagation of errors method (Topping, 1972):

$$PER = \sqrt{\sum_{i=1}^{n}(E_1^2 + E_2^2 + E_3^2 + E_4^2)} \quad (9)$$

where PER = probable error range (±%); n = number of potential error sources; and E_1, E_2, E_3, and E_4 are uncertainties (%) associated with flow measurement, sample collection, sample storage, and laboratory analysis, respectively. In hydrology, this method has been used for uncertainty estimates related to discharge measurements (Sauer and Meyer, 1992) and water quality (Cuadros-Rodriquez et al., 2002; Harmel and Smith, 2007).

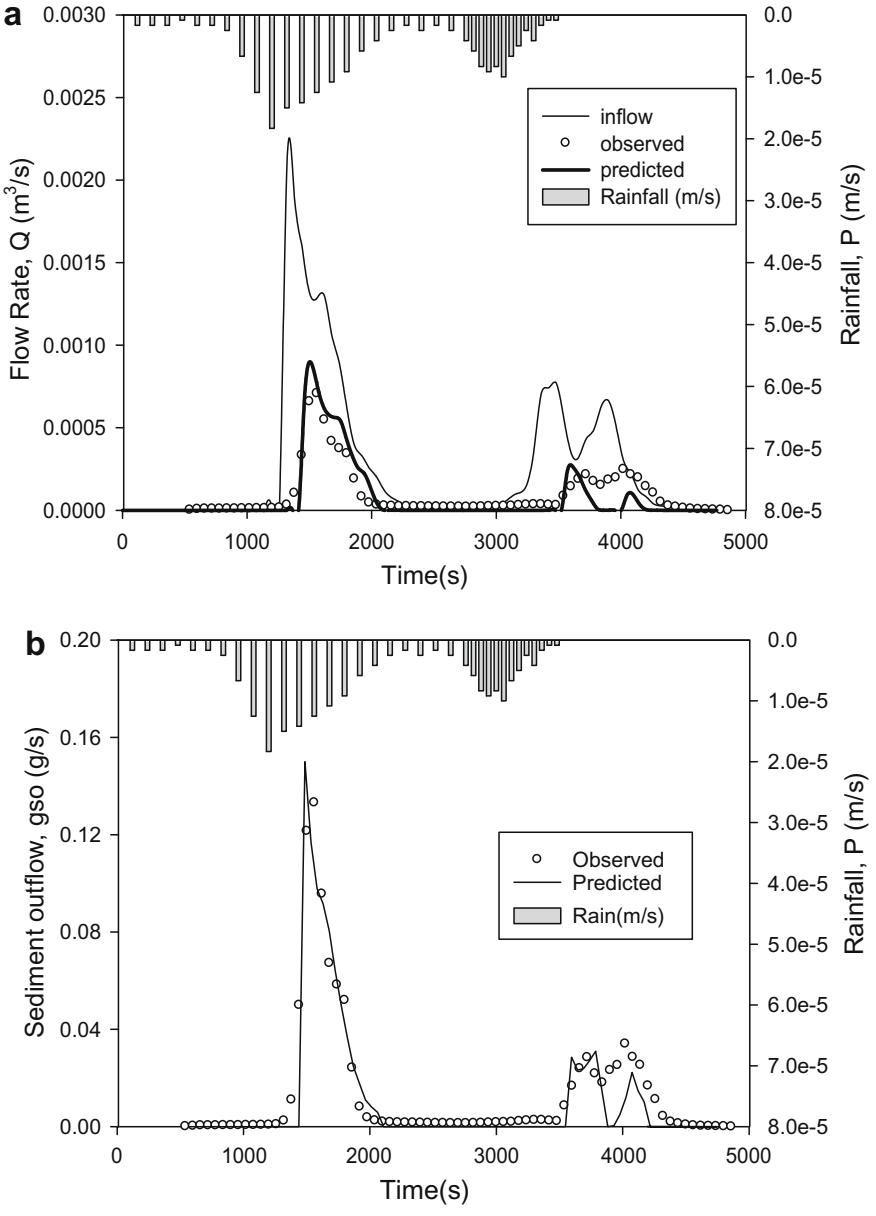

Fig. 2. Hydrograph (a) and sedimentograph (b) for the rainfall–runoff event B071406V3.

Table 7
Goodness-of-fit indicators for runoff hydrographs and sediment pollutographs simulations in with and without including uncertainty of measured data (PER = ± 20% for hydrology, PER = ±29% for sediment).

Event ID	Runoff						Sediment					
	PER = 0%			PER = 20%			PER = 0%			PER = 29%		
	C_{eff}	C_{eff_m}	$RMSE$[b]	C_{eff_m}	C_{eff_m}	$RMSE$	C_{eff}	C_{eff_m}	$RMSE$[b]	C_{eff}	C_{eff_m}	$RMSE$
Calibration												
B061306V2[a]	0.564	0.514	0.00001	0.737	0.635	0.00001	0.675	0.622	0.0006	0.842	0.760	0.0005
B071406V3	0.737	0.548	0.00007	0.852	0.690	0.00006	0.762	0.596	0.0122	0.929	0.813	0.0066
B072006V3	0.766	0.657	0.00021	0.905	0.801	0.00013	0.556	0.577	0.0564	0.855	0.768	0.0322
B072806V3	−0.038	0.000	0.00010	0.380	0.241	0.00008	−0.089	0.148	0.0193	0.483	0.404	0.0133
B090606V2	0.986	0.884	0.00004	0.994	0.932	0.00003	0.803	0.730	0.0295	0.948	0.872	0.0152
B090906V2	0.857	0.703	0.00026	0.943	0.848	0.00016	0.700	0.584	0.0928	0.934	0.837	0.0435
B091006V3	0.577	0.595	0.00019	0.738	0.675	0.00014	0.774	0.677	0.0190	0.944	0.853	0.0095
B101206V3	0.791	0.728	0.00011	0.896	0.820	0.00007	0.471	0.572	0.0190	0.845	0.743	0.0103
A020306V3	−0.250	0.202	0.00001	0.223	0.392	0.00001	−3.234	−0.227	0.0002	−2.039	0.046	0.0002
A070706V3	0.733	0.674	0.00002	0.870	0.792	0.00001	0.171	0.421	0.0014	0.770	0.700	0.0007
A072806V3	0.836	0.726	0.00005	0.935	0.829	0.00003	0.203	0.392	0.0066	0.726	0.662	0.0039
A091006V3	−1.044	0.188	0.00002	−0.540	0.345	0.00002	−0.334	0.228	0.0009	0.340	0.455	0.0006
Validation												
B061306V3	−0.248	0.233	0.00002	0.201	0.386	0.00001	−0.162	0.332	0.0012	0.414	0.526	0.0009
B071406V2	0.257	0.379	0.00012	0.449	0.523	0.00011	−0.714	0.016	0.0326	0.482	0.654	0.0179
B072006V2	0.403	0.494	0.00034	0.643	0.636	0.00026	−0.954	0.229	0.1183	−0.118	0.481	0.0894
B072806V2	−1.150	−0.215	0.00015	−0.648	0.026	0.00013	−0.539	−0.025	0.023	0.143	0.243	0.0171
B090606V3	−0.236	0.295	0.00038	0.209	0.436	0.00030	−0.180	0.361	0.0722	0.405	0.546	0.0513
B090906V3	0.645	0.529	0.00041	0.839	0.729	0.00027	0.357	0.436	0.1359	0.865	0.756	0.0623
B091006V2	0.110	0.417	0.00025	0.408	0.595	0.00020	−0.258	0.126	0.0448	0.168	0.331	0.0364
B101206V2	−1.168	0.211	0.00034	−0.805	0.342	0.00031	−2.556	0.030	0.0493	−2.064	0.180	0.0458
A020306V2	−11.61	−0.642	0.00003	−10.65	−0.458	0.00003	−49.76	−1.765	0.0006	−47.80	−1.493	0.0006
A070706V2	0.240	0.442	0.00003	0.518	0.587	0.00002	0.489	0.543	0.0011	0.710	0.698	0.0008
A072806V2	0.480	0.506	0.00008	0.726	0.650	0.00006	0.043	0.347	0.0073	0.662	0.627	0.0043
A091006V2	−3.571	−0.114	0.00003	−2.770	0.056	0.00003	−0.316	0.233	0.0008	0.373	0.468	0.0006

[a] In Event ID, A = Site A; B = Site B; six numbers succession = Gregorian date; V2 = plot number 2 in VFS area. The lengths of V2 and V3 at site A are 4.1 m and 5.8 m, respectively, and at site B are 6.8 m and 13.4 m, respectively.
[b] Units of *RMSE*s in hydrology and sediment are (m^3/s) and (g/s), respectively.

The measured data uncertainty of each error category (E_1–E_4) determined based on the sample collecting and data analyses procedures (Harmel et al., 2006) was summarized in Table 5. Sediment deposited in the flume can result in errors of measured flows (E_1). Thus, flow uncertainty was taken as poor condition (10%) and added up to 20% to account for sediment effect on measurement. Since DP, TP, and sediment were collected from the flow, 20% of measured flow error was chosen. The sampling uncertainty (E_2) of TP was taken as that of sediment since most P in TP comes from mineral apatite in the soil transported as sediment. Storage uncertainty (E_3) of DP was taken as maximum value of the storage error (Kotlash and Chessman, 1998) but was increased up to 45% to account for potential dissolution of carbonate–fluorapatite (CFA, also called francolite), since CFA exists in water/sediment samples. Thereby, probable error ranges (Eq. (9)) were calculated yielding 50%, 30%, 29%, and 20%, for DP, TP, sediment, and flow, respectively (Table 5). The PER was then incorporated into the goodness-of-fit indicators presented in the Appendix section following Harmel and Smith (2007) to evaluate the prediction performances of VFSMOD-W.

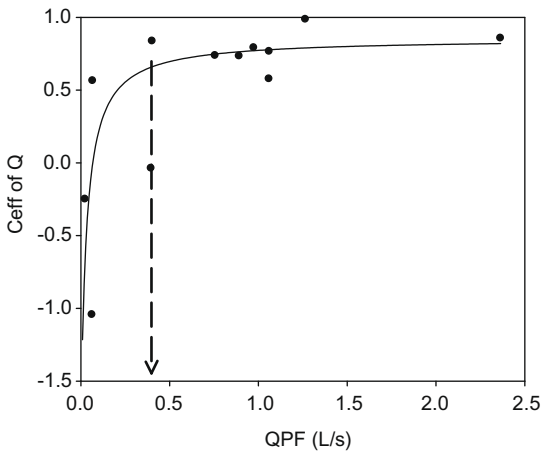

Fig. 3. Comparison of filter strip peak flow measured on the experimental site vs. goodness-of-fit indicator (C_{eff}) of VFSMOD-W runoff predictions.

Table 8
The selected goodness-of-fit indicators for output each quantity with/without including PER.

Quantity	Error range	Calibration			Validation		
		C_{eff}	C_{eff_m}	$RMSE$	C_{eff}	C_{eff_m}	$RMSE$
TRF (m^3)	PER = 0%	0.987	0.863	0.104	0.971	0.837	0.125
	PER = 20%	0.998	0.961	0.042	0.992	0.938	0.067
MSF (kg)	PER = 0%	0.966	0.797	0.031	0.908	0.775	0.030
	PER = 29%	0.995	0.933	0.010	0.984	0.937	0.012
RDR (%)	PER = 0%	0.767	0.461	11.08	0.799	0.598	10.52
	PER = 20%	0.926	0.782	5.698	0.927	0.820	6.689
SDR (%)	PER = 0%	0.928	0.624	0.084	0.851	0.695	0.073
	PER = 29%	0.980	0.830	0.040	0.977	0.904	0.031
PPF (g)	PER = 0%	0.956	0.793	0.876	0.887	0.766	0.922
	PER = 30%	0.990	0.912	0.381	0.970	0.917	0.414
DPF[a] (g)	PER = 0%	0.865	0.672	0.579	0.783	0.701	0.571
	PER = 50%	0.999	0.976	0.039	1.000	0.995	0.005
DPF[b] (g)	PER = 0%	0.982	0.858	0.211	0.993	0.917	0.105
	PER = 50%	1.000	0.991	0.026	1.000	0.997	0.007
TPF[a] (g)	PER = 0%	0.946	0.768	1.332	0.891	0.786	1.293
	PER = 30%	0.991	0.913	0.465	0.998	0.977	0.142
TPF[b] (g)	PER = 0%	0.966	0.810	1.062	0.937	0.819	0.981
	PER = 30%	0.995	0.936	0.375	0.995	0.962	0.257

[a] DP diluted from rainfall.
[b] Rainfall induces the DP released from apatite.

Results and discussion

Optimized value of calibrated parameters

A total of twenty four events (calibration and validation events) were selected to evaluate VFSMOD-W performance in simulating runoff, sediment, and P transport in VFS from refuse mining sand tailings (Table 6). Optimized values of the selected parameters for the 12 calibration events are listed in Table 6. In addition, the measured and predicted quantities for the events are also included. The ranges of optimized VN and VKS for all the events are within the measured parameter ranges for each site (Table 3). The range

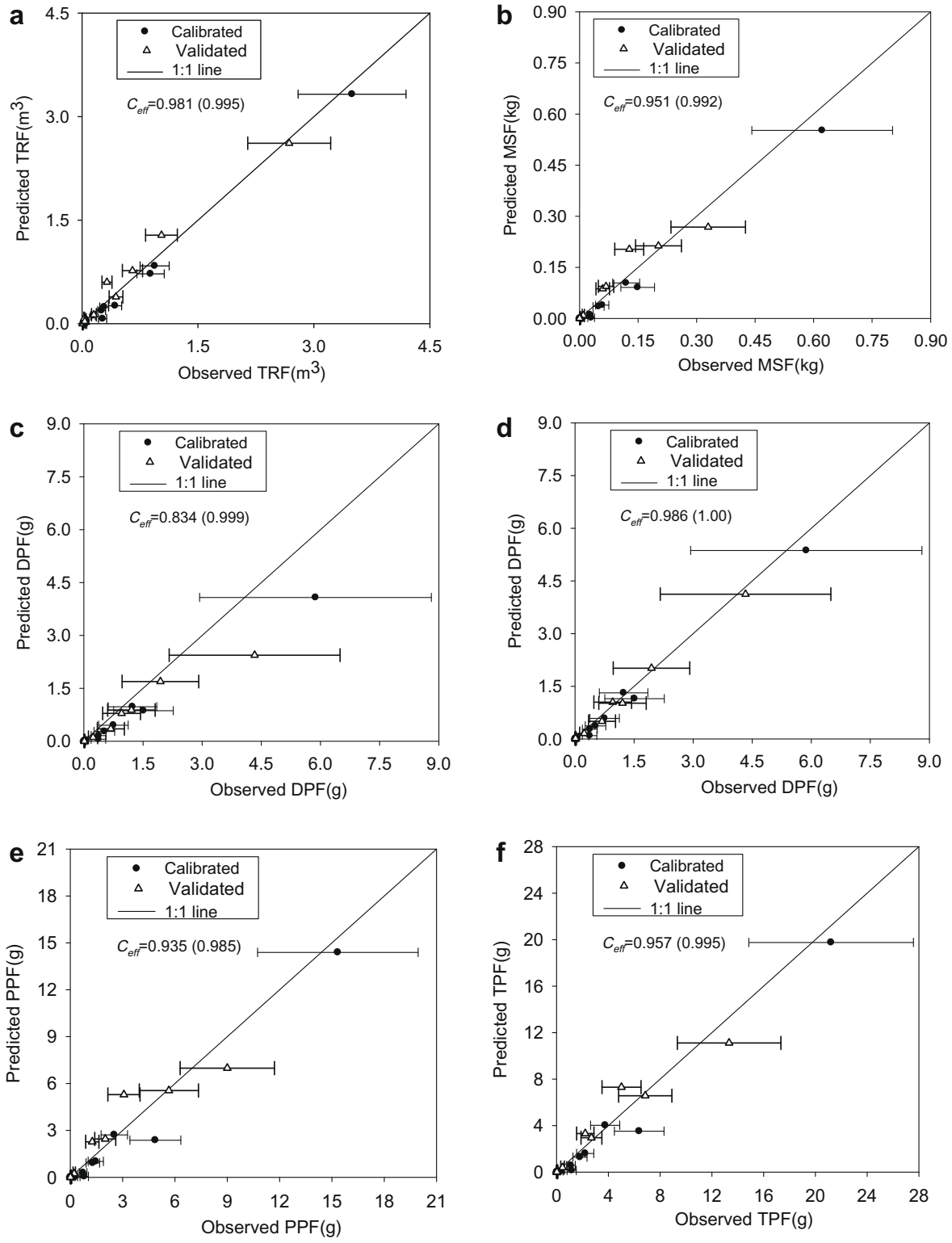

Fig. 4. Scatterplots of measured and predicted runoff, sediment and phosphorus output variables, including measurement uncertainty for each measured value plotted as an error bar. (a) Total runoff output from filter (TRF), (b) Mass of sediment output from filter (MSF); (c) DP mass output from filter (DPF) considering dilution by rainfall; (d) DP mass output from filter (DPF) considering P release from apatite; (e) PP mass output from filter (PPF); (f) TP mass output from filter (TPF; DP fraction considering P release from apatite). C_{eff} including PER is shown in parenthesis.

of optimized OS is within ±15% of measured OS. Optimized RNA for each event is between 0.08 and 0.43, typical of grass with different densities. For each event optimized $d_p > 0.0037$ μm (COARSE > 0.5 as well), which confirms that the experimental area contains a high fraction of sand (>0.94). The optimized values of d_p and COARSE match the experimental measurements from sediment particle size distribution of water samples. As an example Fig. 2 shows observed and predicted hydrographs and sedimentographs of one of the 24 events with a filter sediment trapping efficiency of about 98%. The inflow mass of sediment was two orders of magnitude larger than outflow, thus inflow sediment was not included in the sedimentograph (Fig. 2b). The visual inspection of Fig. 2 indicates a satisfactory match of predicted and observed values.

Evaluation of model calibration and validation results

Hydrology component

Table 7 summarizes the VFSMOD-W performance for simulating runoff and sediment load, expressed as different goodness-of-fit indicators by considering (PER > 0%) and disregarding (PER = 0%) measurement uncertainty. Keeping in mind that peak flow has a significant effect on sediment and runoff transport, and that the C_{eff} is known to be sensitive to large values, we analyzed the C_{eff} obtained for all the 12 calibration events with respect to the observed peak outflow (QPF). A relationship between QPF and C_{eff} of runoff flow simulation was found (Fig. 3), such that smaller events (QPF < 0.0004 m^3/s) were not simulated well with the model ($C_{eff} < 0.60$), likely due to limitations of the experimental system to register such small events. The low flow velocity of these 4 events may have limited energy to flush deposited sediment in the flume. The measured TRFs were less than 0.06 m^3 except for event B072806V3 (Table 6). Under this situation, deposited sediment in the flume may raise the water level and consequently increase the measured flow rate. For the remaining eight events (QPF > 0.0004 m^3/s), VFSMOD-W predicted the measured hydrographs well ($C_{eff} = 0.79 \pm 0.12$; $C_{eff\_m} = 0.69 \pm 0.10$). When considering PER the average C_{eff} increased up to 0.89 ± 0.08 ($C_{eff\_m} = 0.80 \pm 0.08$). In most events C_{eff} is higher than C_{eff_m} for both hydrograph and sedimentograph predictions (Table 7), which indicates that the model can simulate higher flow volumes satisfactorily. The TRF prediction of calibrated events was also very good as shown in Table 8 ($C_{eff} = 0.987$). Although the predicted hydrographs of validation events were not as good ($C_{eff} = 0.10 \pm 0.57$; $C_{eff\_m} = 0.41 \pm 0.11$), VFSMOD-W predicted TRF very well for validated events ($C_{eff} = 0.971$) as shown in Table 8. Consequently, VFSMOD-W predicted TRF very well for the combined dataset of 24 events representing different filter lengths, experimental site conditions, and rainfall intensities as shown in Fig. 4a (C_{eff} and C_{eff} considering the PER are 0.981 and 0.995, respectively). Similarly, C_{eff} (considering the PER) of RDR for these 24 events is about 0.92. Overall, VSFMOD-W was found to successfully predict the efficiency of VFS used to control runoff transport from these phosphate mining areas.

Sediment component

Once VFSMOD-W was tested for runoff, the model also provided good sediment transport predictions. For the events with QPF > 0.0004 m^3/s, the average C_{eff} was 0.63 ± 0.19, and including PER, it increased up to 0.87 ± 0.09 (Table 7). On the other hand, for those events (QPF < 0.0004 m^3/s) where runoff was not well predicted, the measured MSFs were less than 3 g except for event B072806V3. The predicted MSFs were zero in these low runoff events. Thus, similarly to the runoff case, the model performed well throughout the range of measured data, except for the low values of measured runoff subject to experimental limitations. The predicted sediment graphs of validated events were not satisfactory for all events (Table 7). However, VFSMOD-W predicted MSF very well for validated events as shown in Table 8 ($C_{eff} = 0.908$), and also satisfactorily for the 24 events as shown in Fig. 4b (C_{eff} and C_{eff} including the PER are 0.951–0.992, respectively). For predicting SDR, C_{eff} including the PER for these 24 events is about 0.98. Overall, VSFMOD-W was found to successfully predict sediment trapping efficiency of VFS used for controlling sediment transport from phosphate mining sand tailings.

Phosphorus prediction

Measured DP values versus DP computed with the first and second simplified modeling approaches (i.e. by considering or disregarding dilution from rainfall, respectively) for 24 events are represented in Fig. 4c and d. Good DP predictions ($C_{eff} = 0.986$) were found based on the assumption of considering rainfall impact on P release from apatite (Fig. 4d and Tables 6 and 8). The release of DP from apatite into runoff water maintains the system at equilibrium from the DP loss from infiltration and dilution of DP concentration from rainfall. This good prediction in runoff and sediment not only results in good DP predictions, but also in good PP predictions ($C_{eff} = 0.935$ as shown in Fig. 4e) since apatite exists almost uniformly in sediment. The C_{eff} of TP ($C_{eff} = 0.957$ as shown in Fig. 4f) is also as high as PP since DP is a small fraction of TP in most events. The acceptable match between observed and predicted values for PP and TP is shown in Fig. 4e and f.

Goodness-of-fit indicators for different model outputs corresponding to hydrology, sediment, and P transport of all the 24 events are summarized in Table 8. Again, VFSMOD-W was not able to match small events well likely due to the experimental error mentioned above. In these low runoff events the *RMSE*s of sediment are less than 0.0006 g/s. Thus, the small magnitude did not have a significant effect on goodness-of-fit indicators when bigger events were included in the comparison. When including uncertainty of measured data in each quantity for the 24 events, the $C_{eff} > 0.92$ for each output quantity. The C_{eff_m} of each quantity increased also significantly. This means that VFSMOD-W combined with the simplified P transport model was able to predict well the dynamic behavior of runoff, sediment, and P transport for the mining tailings site conditions.

Conclusions

VFSMOD-W was used to model the efficiency of vegetative filter strips for controlling surface runoff pollution from phosphate mining sand tailings. After calibration and validation with 24 rainfall–runoff experimental events, the optimized model parameters were identified within the measured ranges. Model simulations of smaller events (peak flow, QPF < 0.0004 m^3/s) were not successful ($C_{eff} < 0.60$), likely due to limitations of the experimental system to register such small events. For those events (QPF < 0.0004 m^3/s) where runoff simulation was poor, the measured total runoff output volume was less than 0.06 m^3 and measured sediment output mass was less than 3 g. For the remaining events (QPF > 0.0004 m^3/s), satisfactory VFSMOD-W predictions were obtained for runoff ($C_{eff} = 0.79 \pm 0.12$; C_{eff} including PER = 0.89 ± 0.08) and sediment ($C_{eff} = 0.63 \pm 0.12$; C_{eff} including PER = 0.87 ± 0.09). Inclusion of uncertainty of measured data in the goodness-of-fit indicators is a more realistic way to evaluate model performance. Thereby, taking into account the uncertainty of measured data, VFSMOD yielded improved goodness-of-fit indicators for both runoff and sediment predictions. The good model predictions in runoff ($C_{eff} = 0.971$ for TRF) and sediment ($C_{eff} = 0.951$ for MSF), also resulted in good predictions of P ($C_{eff} = 0.957$ for TPF; $C_{eff} = 0.986$ for DPF) transport based on the simplified modeling proposed, where the estimation of DP movement is described by assuming

rainfall impact on P release from apatite. The release of DP from apatite into runoff water maintains the system equilibrium for the DP loss from infiltration and dilution of DP concentration from rainfall. The successful performance of the model indicates that it can be a useful tool for management agencies and consultants involved in mining permitting in Florida's upper Peace River basin to design VFS for controlling runoff and P transport in phosphate mining sand tailings.

Acknowledgments

This research was supported by the FL-DEP, Bureau of Mine Reclamation (Contract No. SP633). We thank Paul Lane, Larry Miller (UF); Kevin Claridge, Michelle Harmeling, Marisa Rhian, Charles Cook, David Arnold, and Michael Elswick (Bureau of Mine Reclamation, DEP, FL) for their support and assistance in installing and maintaining experimental sites. Thanks are also given to Ginqin Yu (TREC, UF), Bill Reve, Lisa Stanley, and Aja Stoppe (UF) for laboratory technical assistance. We also thank Dr. Axel Ritter for attentive review of the manuscript and advice on simulations.

Appendix

Nash and Sutcliffe coefficient of efficiency ($\mathbf{C_{eff}}$)

The Nash and Sutcliffe coefficient of efficiency, C_{eff} (Nash and Sutcliffe, 1970) is widely used to evaluate the performance of hydrologic and water quality models (McCuen et al., 2006; Erpul et al., 2003; Merz and Bloschl, 2004). Here, it is calculated as:

$$C_{eff} = 1 - \sum_{i=1}^{N}(O_i - P_i)^2 \Big/ \sum_{i=1}^{N}(O_i - \bar{O})^2 \quad \text{(a)}$$

where O_i and P_i are the observed and predicted values of the hydrograph or sedimentograph, respectively; $\bar{O}$ is the average value of observed data; and N is the number of time steps of the hydrograph or sedimentograph. The C_{eff} can be sensitive to sample size, outliers, magnitude bias, and time-offset bias (McCuen et al., 2006). The C_{eff} significantly is sensitive to larger values and insensitive to lower values (Legates and McCabe, 1999). Thereby, high C_{eff} values may be obtained even when the fit is relatively poor.

Modified form of C_{eff} (C_{eff_m})

The modified form of C_{eff} was developed by Krause et al. (2005) to reduce the sensitivity of C_{eff} to large values:

$$C_{eff_m} = 1 - \sum_{i=1}^{N}(O_i - P_i)^j \Big/ \sum_{i=1}^{N}(O_i - \bar{O})^j \quad \text{with } j = 1 \quad \text{(b)}$$

Root mean square error (RMSE)

A measure of total error is usually computed as the square root of the sum of the square discrepancies of observed and predicted values.

$$RMSE = \sqrt{N^{-1}\sum_{i=1}^{N}(O_i - P_i)^2} \quad \text{(c)}$$

PER incorporated into the goodness-of-fit indicators

The uncertainty boundaries of the observation were calculated as:

$$UO_i(l) = O_i - PER_i * O_i/100 \text{and} UO_i(u) = O_i + PER_i * O_i/100 \quad \text{(d)}$$

where $UO_i(u)$ = upper uncertainty boundary for each observed data point; $UO_i(l)$ = lower uncertainty boundary for each observed data point; PER_i = probable error range for each measured data point. In this study, we assume that all measured data of each category have the same PER during each event.

To include the PER into the goodness-of-fit indicators the deviation term ($e_i = O_i - P_i$) in Eqs. (a, b) in Appendix was replaced by the modified deviation, em_i, which is defined based on the PER of the measured value and model predicted value. When a predicted value is located outside the uncertainty boundaries, the deviation is calculated as the difference between the predicted value and the nearest uncertainty boundary; otherwise, the deviation is equal to 0:

$$em_i = 0 \quad \text{for } UO_i(l) \leqslant P_i \leqslant UO_i(u) \quad \text{(e)}$$

$$em_i = UO_i(l) - P_i \quad \text{for } P_i < UO_i(l) \quad \text{(f)}$$

$$em_i = UO_i(u) - P_i \quad \text{for } P_i > UO_i(u) \quad \text{(g)}$$

References

Abu-Zreig, M., Rudra, R.P., Whiteley, H., 2001. Validation of a vegetated filter strip model (VFSMOD). Hydrol. Process. 15, 729–742.
Barfield, B.J., Toller, E.W., Hayes, F.C., 1978. The Use of Grass Filters for Sediment Control in Strip Mining Drainage. I: Theoretical Studies on Artificial Media. Publish No. 35-RRR2–78. Institute for Mining and Minerals Research, University of Kentucky, Lexington.
Barfield, B.J., Tollner, E.W., Hayes, J.C., 1979. Filtration of sediment by simulated vegetation I. Steady-state flow with homogeneous sediment. Trans. ASAE 22, 540–545.
Beven, K., 2006. On undermining the science? Hydrol. Process. 20, 1–6.
Cuadros-Rodriquez, L., Hernandez Torres, M.E., Almansa Lopez, E., Egea Gonzalez, F.J., Arrebola Liebanas, F.J., Martinez Vidal, J.L., 2002. Assessment of uncertainty in pesticide multiresidue analytical methods: main sources and estimation. Anal. Chim. Acta 454, 297–314.
Dane, J.H., Topp, G.C., 2002. Methods of soils analysis, part 4. Soil Science Society of America Book Series vol. 5, pp. 1692.
Dillaha, T.A., Reneau, R.B., Mostaghimi, S., Lee, D., 1989. Vegetative filter strips for agricultural nonpoint source pollution control. Trans. ASAE 32, 491–496.
Dosskey, M.G., Eisenhauer, D.E., Helmers, M.J., 2005. Establishing conservation buffers using precision information. J. Soil Water Conserv. 60 (6), 349–354.
Dosskey, M.G., Helmers, M.J., Eisenhauer, D.E., 2006. An approach for using soil surveys to guide the placement of water quality buffers. J. Soil Water Conserv. 61 (6), 344–354.
Dosskey, M.G., Helmers, M.J., Eisenhauer, D.E., 2008. A design aid for determining width of filter strips. J. Soil Water Conserv. 63 (4), 232–241.
Erpul, G., Norton, L.D., Gabriels, D., 2003. Sediment transport from interrill areas under wind-driven rain. J. Hydrol. 276, 184–197.
Foster, G.R., Lane, L.J., Nowlin, J.D., Laflen, J.M., Young, R.A., 1980. A model to estimate sediment yield from field-sized areas development of model. In: Knisel, W.G. (Ed.), CREAMS: A Field-Scale Model for Chemical, Runoff, and Erosion from Agricultural Management Systems, vol. II. USDA – Science Education Administration Conservation Report 26, pp. 193–281.
Fox, A.L., Eisenhauer, D.E., Dosskey, M.G., 2005. Modeling water and sediment trapping by vegetated filters using VFSMOD: comparing methods for estimating infiltration parameters. ASAE Paper No. 052118. ASAE, St. Joseph, MI.
Gao, B., Walter, M.T., Steenhuis, T.S., Hogarth, W.L., Parlange, J.Y., 2004. Rainfall induced chemical transport from soil to runoff: theory and experiments. J. Hydrol. 295, 291–304.
Gharabaghi, B., Rudra, R.P., Whiteley, H.R., Dickinson, W.T., 2000. Improving removal efficiency of vegetative filter strips. ASAE Paper No. 00-2083. ASAE, St. Joseph, MI.
Gordon, J.D., Newland, C.A., Gagliardi, S.T., 2000. Laboratory performance in the sediment laboratory quality-assurance project 1996-98. US Geological Survey, Water Resources Investigations Report 99-4184, Washington, DC.
Haan, C.T., Barfield, B.J., Hayes, J.C., 1994. Design hydrology and sedimentology for small catchments. Academic Press, San Diego, CA.
Han, J., Wu, S., Allan, C., 2005. Suspended sediment removal by vegetative filter strip treating highway runoff. J. Environ. Sci. Health. 40, 1637–1649.
Harmel, R.D., Smith, P.K., 2007. Consideration of measurement uncertainty in the evaluation of goodness-of-fit in hydrologic and water quality modeling. J. Hydrol. 337, 326–336.
Harmel, R.D., Cooper, R.J., Slade, R.M., Haney, R.L., Arnold, J.G., 2006. Cumulative uncertainty in measured streamflow and water quality data for small watersheds. Trans. ASABE 49, 689–701.
Huyer, W., Neumaier, A., 1999. Global optimization by multilevel coordinate search. J. Global Optim. 14, 331–355.
Kalin, L., Hantush, M.M., 2003. Evaluation of sediment transport models and comparative application of two watershed models. US Environmental Protection Agency. National Risk Management Research Laboratory, Cincinnati, OH. EPA 600/R-03/139.
Kizil, U., Disrud, L.A., 2002. Vegetative filter strips modeling of a small watershed. ASAE Paper No. 022133. ASAE, St. Joseph, MI.

Kotlash, A.R., Chessman, B.C., 1998. Effects of water sample preservation and storage on nitrogen and phosphorus determinations: implications for the use of automated sampling equipment. Water Res. 32, 3731–3737.

Krause, P., Boyle, D.P., Bäse, F., 2005. Comparison of different efficiency criteria for hydrological model assessment. Adv. Geosci. 5, 89–97.

Kuo, Y.M., 2007. Vegetative filter strips to control surface runoff phosphorus transport from mining sand tailings in the upper peace river basin of Central Florida. Ph.D. Dissertation, University of Florida. <http://purl.fcla.edu/fcla/etd/UFE0021212> (accessed July 2009).

Kuo, Y.M., Muñoz-Carpena, R., Li, Y.C., Campbell, K.L., Parsons, J.E., 2005. Using Vegetative Filter Strips to Reduce Phosphorus Transport from the Phosphorus Mining Areas in Central Florida. ASAE Paper No. 05-2174. ASAE, St. Joseph, MI.

Kuo, Y.-M., W.G. Harris, R. Muñoz-Carpena, R.D. Rhue, Y. Li. 2009. Apatite control of phosphorus release to runoff from soils of phosphate mine reclamation areas. Water, Air & Soil Pollution. doi:10.1007/s11270-008-9969-4.

Lambot, S., Javaux, M., Hupet, F., Vanclooster, M., 2002. A global multilevel coordinate search procedure for estimating the unsaturated soil hydraulic properties. Water Resour. Res. 38 (11), 1224.

Legates, D.R., McCabe, G.J., 1999. Evaluating the use of "goodness-of-fit" measures in hydrologic and hydroclimatic model validation. Water Resour. Res. 35, 233–241.

Martin, G.R., Smoot, J.L., White, K.D., 1992. A comparison of surface-grab and cross-sectionally integrated stream-water-quality sampling methods. Water Environ. Res. 64, 866–876.

McCuen, R.H., Knight, Z., Cutter, A.G., 2006. Evaluation of the Nash–Sutcliffe efficiency index. J. Hydrol. Eng. 11, 597–602.

Mercurio, G., Perot, J., Roth, N., Southerland, M., 2002. Maryland biological stream survey 2000: quality assessment report. Springfield, VA.: Versar, Inc., Baltimore. MD: Maryland Department of Natural Resources.

Merz, R., Bloschl, G., 2004. Regionalization of catchment model parameters. J. Hydrol. 287, 95–123.

Millington, R.J., Quirk, J.P., 1960. Transport in porous media. In: Transactions of the 7th International Congress of Soil Science, vol. 1. Madison, WI, pp. 97–106.

Mueller, D.K., Hamilton, P.A., Helsel, D.R., Hitt, K.J., Ruddy, B.C., 1995. Nutrients in ground water and surface water of the United States – an analysis of data through 1992. US Geological Survey, Water Resources Investigations Report 95-4031. pp. 74.

Muñoz-Carpena, R., Miller, C.T., Parsons, J.E., 1993a. A quadratic Petrov–Galerkin solution for kinematic wave overland flow. Water Environ. Res. 29, 2615–2627.

Muñoz-Carpena, R., Parsons, J.E., Gilliam, J.W., 1993b. Numerical approach to the overland flow process in vegetative filter strips. Trans. ASAE 36, 761–770.

Muñoz-Carpena, R., Parsons, J.E., Gilliam, J.W., 1999. Modeling hydrology and sediment transport in vegetative filter strips. J. Hydrol. 214, 111–129.

Muñoz-Carpena, R., Zajac, Z., Kuo, Y.M., 2007. Evaluation of water quality models through global sensitivity and uncertainty analyses techniques: application to the vegetative filter strip model VFSMOD–W. Trans. ASABE 50 (5), 1719–1732.

Nash, J.E., Sutcliffe, J.V., 1970. River flow forecasting through conceptual models. Part 1 – a discussion of principles. J. Hydrol. 10, 282–290.

Nelder, J.A., Mead, R., 1965. A simplex method for function minimization. Comput. J. 7, 308–313.

Poletika, N.N., Coody, P.N., Fox, G.A., Sabbagh, G.J., Dolder, S.C., White, J., 2009. Chlorpyrifos and atrazine removal from runoff by vegetated filter strips: experiments and predictive modeling. J. Environ. Qual. 38 (3), 1042–1052.

Ritter, A., Hupet, F., Muñoz-Carpena, R., Vanclooster, M., Lambot, S., 2003. Using inverse methods for estimating soil hydraulic properties from field data as an alternative to direct methods. Agric. Water Manage. 59, 77–96.

Ritter, A., Muñoz-Carpena, R., Pérez-Ovilla, O., 2007. An inverse calibrator for VFSMOD-W using the Global Multilevel Coordinate Search/Nelder–Mead Simplex algorithm. ASAE Paper No 02-2212. ASAE, St. Joseph, MI.

Rudra, R.P., Gupta, N., Sebti, S., Gharabaghi, B., 2002. Incorporation of a phosphorus component to the upland hydrology module of the VFSMOD model. ASAE Paper No. 02-2078. ASAE, St. Joseph, MI.

Sabbagh, G.J., Fox, G.A., Kamanzi, A., Roepke, B., Tang, J.Z., 2009. Effectiveness of vegetative filter strips in reducing pesticide loading: quantifying pesticide trapping efficiency. J. Environ. Qual. 38 (2), 762–771.

Sauer, V.B., Meyer, R.W., 1992. Determination of error in individual discharge measurements. US Geological Survey, Open File Report 92-144. Washington, DC.

Tollner, E.W., Barfield, B.J., Haan, C.T., Kao, T.Y., 1976. Suspended sediment filtration capacity of simulated vegetation. Trans. ASAE 19, 678–682.

Tomer, M.D., Dosskey, M.G., Burkart, M.R., James, D.E., Helmers, M.J., Eisenhauer, D.E., 2009. Methods to prioritize placement of riparian buffers for improved water quality. Agrofor. Syst. 75 (1), 17–25.

Topping, J., 1972. Errors of Observation and Their Treatment. Chapman and Hall, London, UK.

UNEP, 2001. Environmental aspects of phosphate and potash mining. United Nations Environment Programme, International Fertilizer Industry Association.

USDA-NRCS, 1976. Field office technical guide, section IV—practice standards and specifications, 342—critical area planting.

USEPA, 2000. Water quality criteria for nitrogen and phosphorus pollution, EPA 822-B-00-021, Office of Water (4304), Washington, DC. <http://www.epa.gov/waterscience/criteria/nutrient/ecoregions/rivers/rivers_12.pdf> (accessed 02 April 2008).

USEPA, 2005. Management measures to protect and restore wetlands and riparian areas for the abatement of nonpoint source pollution. Chapter 6: management measure for vegetated treatment systems. <http://www.epa.gov/owow/nps/wetmeasures>. (accessed 02 June 2007).

White, M.J., Arnold, J.G., 2009. Development of a simplistic vegetative filter strip model for sediment, nutrient retention at the field scale. Hydrol. Process. 23, 1602–1616.

Workman, S.R., Skaggs, R.W., 1990. PREFLO: a water management model capable of simulating preferential flow. Trans. ASAE 33 (6), 1939–1948.

Yang, W., Weersink, A., 2004. Cost-effective targeting of riparian buffers. Can. J. Agric. Econ. 52, 17–34.

Zhang, Q., Okoren, C.G., Mankin, K.R., 2001. Modeling fecal pathogen transport in vegetative filter strips. ASAE paper No 01-2194. ASAE, St. Joseph, MI.